Hindawi
Wireless Communications and Mobile Computing
Volume 2021, Article ID 5519786, 9 pages
https://doi.org/10.1155/2021/5519786

Research Article

Spatial Property of Optical Wave Propagation through Anisotropic Atmospheric Turbulence

Bing Guan,[1] Haiyang Yu,[1] Wei Song ,[2] and Jaeho Choi[3]

[1] *School of Computer Science and Engineering, Huizhou University, Huizhou 516007, China*
[2] *Department of Electronic Information and Communication Engineering, Applied Technology College of Soochow University, Suzhou 215325, China*
[3] *Department of Electronic Engineering, CAIIT, Jeonbuk National University, Jeonju 54896, Republic of Korea*

Correspondence should be addressed to Wei Song; songw3015@suda.edu.cn

Received 31 January 2021; Revised 10 June 2021; Accepted 22 November 2021; Published 21 December 2021

Academic Editor: Xiangjie Kong

For the free-space optical (FSO) communication system, the spatial coherence of a laser beam is influenced obviously as it propagates through the atmosphere. This loss of spatial coherence limits the degree to which the laser beam is collimated or focused, resulting in a significant decrease in the power level of optical communication and radar systems. In this work, the analytic expressions of wave structure function for plane and spherical wave propagation through anisotropic non-Kolmogorov turbulence in a horizontal path are derived. Moreover, the new expressions for spatial coherence radius are obtained considering different scales of atmospheric turbulence. Using the newly obtained expressions for the spatial coherent radius, the effects of the inner scales and the outer scales of the turbulence, the power law exponent, and the anisotropic factor are analyzed. The analytical simulation results show that the wave structure functions are greatly influenced by the power law exponent α, the anisotropic factor ζ, the turbulence strength $\tilde{\sigma}_R^2$, and the turbulence scales. Moreover, the spatial coherence radiuses are also significantly affected by the anisotropic factor ζ and the turbulence strength $\tilde{\sigma}_R^2$, while they are gently influenced by the power law exponent α and the inner scales of the optical waves.

1. Introduction

In recent years, the traffic carried by the telecommunication network is growing significantly, especially the wireless network. The popularity of wireless data and mobile Internet is much faster than anyone imagined, and it enhances voice communication with much richer multimedia content. Mobile data traffic and mobile service spectrum have increased by many orders of magnitude from 2010 to 2020 [1]. This is an important topic of the sixth generation (6G) wireless communication. On 6G communication, optical wireless communication (OWC) technology has many advantages in frequency spectrum, security, and transmission rate, which can be used as a potential replacement and supplement of radio frequency-based wireless communication technology. OWC technology provides a basic combination of the various advantages necessary to deliver high-speed services to optical backbone networks. It provides an unlicensed spectrum, almost unlimited data rate, low-cost development, and convenient installation [2]. On the other hand, the ground-based point-to-point OWC system, also known as free-space optical (FSO) communication system, works at near-infrared frequency. Beam spreading caused by atmospheric turbulence occupies a very important position in FSO communication systems, because it determines the loss of power at the receiver plane [3]. For optical wave propagation, the classic Kolmogorov model has been widely used in theoretical researches due to its simple mathematical form [3–5]. Over the years, the Kolmogorov model is extended and several non-Kolmogorov turbulence models have been also proposed [6–13]. Toselli et al. [6] is one of them, and they analyze the angle of arrival fluctuations by using the generalized exponent factor α instead of the standard exponent value 11/3. The anisotropic factor is also used to describe anisotropy of the atmosphere turbulence [7], and the generalized non-Kolmogorov von Karman spectrum of the anisotropic atmospheric turbulence is available [8–10]. In addition, there are also numerous studies on beam wanders, loss of spatial coherence, temporal frequency spread, and the angle of arrival fluctuation [14–21], which are all related to the random fluctuation of optical waves propagating through random media.

Lately, more research attention is drawn to the theoretical survey of wave structure function (WSF) for the long-exposure modulation transfer function (MTF) and spatial coherence radius (SCR) [22–29]. Based on the Rytov approximation method, a researcher like Young proposes new expressions for the WSFs of optical waves, which fit the moderate to strong fluctuation regimes [22, 23]. Lu et al. have derived new expressions for the WSFs and the SCRs for plane waves and spherical waves propagating through homogeneous and isotropic oceanic turbulence [25]. Moreover, Cui et al. consider the turbulence scales and have derived the long-exposure MTFs for plane waves and spherical waves propagating through anisotropic non-Kolmogorov atmospheric turbulence [26, 27]; Kotiang and Choi and Guan et al. also have derived a new long-exposure MTF for Gaussian waves propagating through isotropic non-Kolmogorov atmospheric turbulence and anisotropic maritime turbulence [28, 29].

In this study, we derive new WSF and SCR expressions for the plane waves and the spherical waves which propagate in the anisotropic non-Kolmogorov atmosphere turbulence. Here, the generalized von Karman model is used by incorporating the anisotropic factor $\zeta^{2-\alpha}$. In the simulation analyses, using the newly derived WSF and SCR expressions, the effects of the inner scale and the outer scale of the eddy size are investigated. In addition to the influences of the power law exponent, the turbulence strength and the anisotropic factor, which are all affecting parameters of the WSFs and SCRs, are also carefully analyzed.

2. Anisotropic Non-Kolmogorov Spectrum with Inner and Outer Scales

Stribling et al. [30] developed a power spectrum in non-Kolmogorov turbulence as the power law for the spectrum of the index of refraction fluctuations is varied from 3 to 4. This power spectrum, which we call the conventional isotropic non-Kolmogorov spectrum:

$$\begin{aligned}\Phi_n(\kappa,\alpha) &= A(\alpha)\tilde{C}_n^2\kappa^{-\alpha}\ (\kappa>0, 3<\alpha<4),\\ A(\alpha) &= \frac{\Gamma(\alpha-1)}{4\pi^2}\cos\left(\frac{\alpha\pi}{2}\right),\end{aligned} \tag{1}$$

where $\Gamma(\cdot)$ is the gamma function, κ is the spatial wave number, α is the power law exponent, and $\tilde{C}_n^2$ is the generalized structure parameter with $m^{3-\alpha}$ as its unit. The function $A(\alpha)$ maintains the consistency between the index structure function and its power spectrum.

Toselli in [7] proposed a new power spectrum by introducing an effective anisotropic parameter ζ. When there are non-Kolmogorov power law and anisotropy along the propagation direction, it is helpful to simulate optical turbulence. Also, the concept of atmospheric turbulence anisotropy at different scales is introduced:

$$\begin{aligned}\Phi_n(\kappa,\alpha,\zeta) &= A(\alpha)\tilde{C}_n^2\zeta^2\left[\zeta^2\kappa_{xy}^2+\kappa_z^2+\kappa_0^2\right]^{-\alpha/2}\\ &\cdot\ \exp\left(-\frac{\zeta^2\kappa_{xy}^2+\kappa_z^2}{\kappa_m^2}\right)(\kappa>0, 3<\alpha<4),\end{aligned} \tag{2}$$

where ζ is the anisotropic factor; $\kappa_0=2\pi/L_0$ and L_0 is the outer scale parameter; $\kappa_m=C(\alpha)/l_0$ and l_0 is the inner scale parameter; $\kappa=\sqrt{\zeta^2(\kappa_x^2+\kappa_y^2)+\kappa_z^2}=\sqrt{\zeta^2\kappa_{xy}^2+\kappa_z^2}$ and κ_x, κ_y, and κ_z are the components of κ in $x, y,$ and z direction; and $C(\alpha)=[\Gamma((5-\alpha)/2)A(\alpha)2/3\pi]^{1/(\alpha-5)}$.

In this case, Equation (2) can be defined as the one in [6], which is formed by multiplying the generalized von Karman model with the anisotropic factor $\zeta^{2-\alpha}$. The resulting expression is then the modified anisotropic non-Kolmogorov power spectrum, and it is defined as follows [31]:

$$\begin{aligned}\Phi_n(\kappa,\alpha,\zeta) &= A(\alpha)\tilde{C}_n^2\zeta^{2-\alpha}\left[\kappa^2+\tilde{\kappa}_0^2\right]^{-\alpha/2}\\ &\cdot\ \exp\left(-\frac{\kappa^2}{\tilde{\kappa}_m^2}\right)(\kappa>0, 3<\alpha<4),\end{aligned} \tag{3}$$

where $\tilde{\kappa}_0^2=\kappa_0^2/\zeta^2$ and $\tilde{\kappa}_m^2=\kappa_m^2/\zeta^2$.

3. The Expressions for Wave Structure Functions

In order to evaluate the performance of optical wave structure function and spatial coherence radius in atmospheric turbulence, we need to derive the wave structure function of optical waves first. In this paper, we first derive the wave structure function of plane wave and spherical wave and then use these equations to derive their spatial coherence radius.

3.1. The Plane Wave Structure Function. The WSF of optical waves propagating in isotropic non-Kolmogorov turbulence is proposed in [3], and it can be used to calculate the spatial coherence radius of the optical waves; the formulae are shown as follows:

$$D_{\mathrm{pl}}(\rho,\alpha)=8\pi^2k^2L\int_0^\infty\kappa\Phi_n(\kappa,\alpha)[1-J_0(\kappa\rho)]d\kappa, \tag{4}$$

$$D_{\mathrm{sp}}(\rho,\alpha)=8\pi^2k^2L\int_0^1\int_0^\infty\kappa\Phi_n(\kappa,\alpha)[1-J_0(\kappa\xi\rho)]d\kappa d\xi, \tag{5}$$

where $D_{\mathrm{pl}}(\rho,\alpha)$ is the plane wave structure function; $D_{\mathrm{sp}}(\rho,\alpha)$ is the spherical wave structure function; ρ is the scalar separation distance between two points in the 2D plane; $k=2\pi/\lambda$ is the optical wave number; $\xi=1-z/L$ and L is the path length; z is the propagation distance; and $J_0(\cdot)$ is the zero-order Bessel function of the first kind.

In this paper, Equation (3) is used as the expression for the anisotropic non-Kolmogorov power spectrum in our derivation of new wave structure function expressions for optical waves. Then, Equations (4) and (5) can be rewritten as follows:

$$D_{\mathrm{pl}}(\rho,\alpha,\zeta)=8\pi^2k^2L\int_0^\infty \kappa\Phi_n(\kappa,\alpha,\zeta)[1-J_0(\kappa\rho)]d\kappa, \tag{6}$$

$$D_{\mathrm{sp}}(\rho,\alpha,\zeta)=8\pi^2k^2L\int_0^1\int_0^\infty \kappa\Phi_n(\kappa,\alpha,\zeta)[1-J_0(\kappa\xi\rho)]d\kappa d\xi. \tag{7}$$

By substituting Equation (3) into Equation (6) and expanding $J_0(\cdot)$ as a series representation, one can obtain the new WSF expression for the plane waves as follows:

$$\begin{aligned}D_{\mathrm{pl}}(\rho,\alpha,\zeta)&=8\pi^2k^2LA(\alpha)\tilde{C}_n^2\zeta^{2-\alpha}\sum_{n=1}^{\infty}\frac{(-1)^{n-1}}{n!\cdot(1)_n}\cdot\left(\frac{\rho}{2}\right)^{2n}\\&\times\int_0^\infty \kappa^{2n+1}\left[\kappa^2+\tilde{\kappa}_0^2\right]^{-\alpha/2}\cdot\exp\left(-\frac{\kappa^2}{\tilde{\kappa}_m^2}\right)d\kappa.\end{aligned} \tag{8}$$

Here, the integration can be resolved by using the confluent hypergeometric function of the second kind defined as follows [32]:

$$U(a,c,z)=\frac{1}{\Gamma(a)}\int_0^\infty e^{-zt}t^{a-1}(1+t)^{c-a-1}dt,\quad a>0,\mathrm{Re}\,(z)>0, \tag{9}$$

$$U(a,c,z)\approx\frac{\Gamma(1-c)}{\Gamma(1+a-c)}+\frac{\Gamma(c-1)}{\Gamma(a)}z^{1-c},\quad |z|<<1. \tag{10}$$

Then, Equation (8) can be derived as follows:

$$\begin{aligned}D_{\mathrm{pl}}(\rho,\alpha,\zeta)&=4\pi^2k^2LA(\alpha)\tilde{C}_n^2\zeta^{2-\alpha}\sum_{n=1}^{\infty}\frac{(-1)^{n-1}}{n!\cdot(1)_n}\cdot\left(\frac{\rho}{2}\right)^{2n}\tilde{\kappa}_0^{2n+2-\alpha}\\&\times\left\{\frac{n!(-1)^n\Gamma(\alpha/2-1)}{(2-\alpha/2)_n\Gamma(\alpha/2)}+\left(1-\frac{\alpha}{2}\right)_n\Gamma\left(1-\frac{\alpha}{2}\right)\frac{\tilde{\kappa}_0^{\alpha-2n-2}}{\tilde{\kappa}_m^{\alpha-2n-2}}\right\}.\end{aligned} \tag{11}$$

Finally, the new expression of the wave structure function for the plane waves is defined as follows:

$$\begin{aligned}D_{\mathrm{pl}}(\rho,\alpha,\zeta)&=4\pi^2k^2LA(\alpha)\tilde{C}_n^2\zeta^{2-\alpha}\left\{\tilde{\kappa}_m^{2-\alpha}\Gamma\left(1-\frac{\alpha}{2}\right)[1-J(\alpha)]\right.\\&\left.+\frac{\rho^2\tilde{\kappa}_0^{4-\alpha}}{(\alpha-2)(\alpha-4)}\right\},\end{aligned} \tag{12}$$

$$J(\alpha)={}_1F_1\left(1-\frac{\alpha}{2};1;-\frac{\rho^2\tilde{\kappa}_m^2}{4}\right), \tag{13}$$

where ${}_1F_1(\cdot)$ is the confluent hypergeometric function of the first kind [32].

3.2. The Spherical Wave Structure Function. By substituting Equation (3) into Equation (7) and expanding $J_0(\cdot)$ as a series representation, one can obtain the new expression of the wave structure function for the spherical waves. It is expressed as follows:

$$\begin{aligned}D_{\mathrm{sp}}(\rho,\alpha,\zeta)&=8\pi^2k^2LA(\alpha)\tilde{C}_n^2\zeta^{2-\alpha}\sum_{n=0}^{\infty}\frac{(-1)^{n-1}}{n!(1)_n}\left(\frac{\rho}{2}\right)^{2n}\\&\times\int_0^1\xi^{2n}d\xi\int_0^\infty\kappa^{2n+1}\left[\kappa^2+\tilde{\kappa}_0^2\right]^{-\alpha/2}\\&\cdot\exp\left(-\frac{\kappa^2}{\tilde{\kappa}_m^2}\right)d\kappa d\xi.\end{aligned} \tag{14}$$

Using Equations (9) and (10), the final expression of the WSF for the spherical waves can be derived and it is rewritten as follows:

$$\begin{aligned}D_{\mathrm{sp}}(\rho,\alpha,\zeta)&=4\pi^2k^2LA(\alpha)\tilde{C}_n^2\zeta^{2-\alpha}\left\{\tilde{\kappa}_m^{2-\alpha}\Gamma\left(1-\frac{\alpha}{2}\right)[1-K(\alpha)]\right.\\&\left.+\frac{\rho^2\tilde{\kappa}_0^{4-\alpha}}{3(\alpha-2)(\alpha-4)}\right\},\end{aligned} \tag{15}$$

$$K(\alpha)={}_2F_2\left(\frac{1}{2},1-\frac{\alpha}{2};\frac{3}{2},1;-\frac{\rho^2\tilde{\kappa}_m^2}{4}\right), \tag{16}$$

where ${}_pF_q(\cdot)$ is the generalized hypergeometric function and p and q are nonnegative integers [32].

4. New Expressions for Spatial Coherence Radius

The main purpose of this section is to calculate the spatial coherence radius of the optical waves. It is used to determine the spatial coherence radius of the wave at the receiver pupil plane. As we know, the spatial coherence radius defines the effective receiver aperture size in a heterodyne detection system. The new expressions for SCRs of the plane waves and the spherical waves are derived in this section. The SCR derivations begin with the new WSFs derived in the previous section. Those WSFs need to be approximated and simplified to be used effectively in numerical computations when one performs computer simulations.

Consider the WSFs in Equations (12) and (15). Those equations involve the confluent hypergeometric functions ${}_1F_1(\cdot)$ and ${}_2F_2(\cdot)$. Those hypergeometric function can be approximately expressed as follows [32]:

$${}_1F_1(a;c;-z)\approx\begin{cases}1-\dfrac{az}{c}, & |z|<<1,\\ \dfrac{\Gamma(c)}{\Gamma(c-a)}z^{-a}, & \mathrm{Re}\,(z)>>1,\end{cases} \tag{17}$$

$$ {}_2F_2(a, b; c, d; -z) \approx \begin{cases} 1 - \dfrac{abz}{cd}, & |z|<<1, \\ \dfrac{\Gamma(c)\Gamma(d)\Gamma(b-a)}{\Gamma(b)\Gamma(c-a)\Gamma(d-a)} z^{-a} + \dfrac{\Gamma(c)\Gamma(d)\Gamma(a-b)}{\Gamma(a)\Gamma(c-b)\Gamma(d-b)} z^{-b}, & \mathrm{Re}\,(z)>>1. \end{cases} \quad (18) $$

Equations (17) and (18) can be substituted into Equations (12) and (15), respectively. The WSFs of the optical waves can be rewritten as follows:

$$ D_{\mathrm{pl}}(\rho, \alpha, \zeta) \approx \begin{cases} R(\alpha)\tilde{\sigma}_R^2(\alpha)\left[\tilde{\kappa}_m^{2-\alpha}\Gamma\left(1-\dfrac{\alpha}{2}\right) - \dfrac{2^{2-\alpha}\Gamma(1-\alpha/2)}{\Gamma(\alpha/2)}\rho^{\alpha-2} - \dfrac{\rho^2\tilde{\kappa}_0^{4-\alpha}}{(\alpha-2)(4-\alpha)}\right], & \rho>>l_0, \\ R(\alpha)\tilde{\sigma}_R^2(\alpha)\rho^2\left[\dfrac{2-\alpha}{8}\tilde{\kappa}_m^{4-\alpha}\Gamma\left(1-\dfrac{\alpha}{2}\right) - \dfrac{\tilde{\kappa}_0^{4-\alpha}}{(\alpha-2)(4-\alpha)}\right], & \rho<<l_0, \end{cases} \quad (19) $$

$$ D_{\mathrm{sp}}(\rho, \alpha, \zeta) \approx \begin{cases} R(\alpha)\tilde{\sigma}_R^2(\alpha)\left[\tilde{\kappa}_m^{2-\alpha}\Gamma\left(1-\dfrac{\alpha}{2}\right) - \dfrac{2^{2-\alpha}\Gamma(1-\alpha/2)}{(\alpha-1)\Gamma(\alpha/2)}\rho^{\alpha-2} - \dfrac{\rho^2\tilde{\kappa}_0^{4-\alpha}}{3(\alpha-2)(4-\alpha)}\right], & \rho>>l_0, \\ R(\alpha)\tilde{\sigma}_R^2(\alpha)\rho^2\left[\dfrac{2-\alpha}{24}\tilde{\kappa}_m^{4-\alpha}\Gamma\left(1-\dfrac{\alpha}{2}\right) - \dfrac{\tilde{\kappa}_0^{4-\alpha}}{3(\alpha-2)(4-\alpha)}\right], & \rho<<l_0, \end{cases} \quad (20) $$

where

$$ R(\alpha) = -0.5\alpha\left(\sin\frac{\pi\alpha}{4}\right)^{-1}\zeta^{2-\alpha}k^{\alpha/2-1}L^{1-\alpha/2}\left[\Gamma\left(1-\frac{\alpha}{2}\right)\right]^{-1}, \quad (21) $$

and $\tilde{\sigma}_R^2(\alpha)$ is the non-Kolmogorov Rytov variance defined by the plane wave scintillation index in non-Kolmogorov turbulence [33] as follows:

$$ \tilde{\sigma}_R^2(\alpha) = -8\pi^2 A(\alpha)\frac{1}{\alpha}\Gamma\left(1-\frac{\alpha}{2}\right)\tilde{C}_n^2 k^{3-\alpha/2}L^{\alpha/2}\sin\frac{\pi\alpha}{4}. \quad (22) $$

From the WSF of the optical waves, the SCR ρ_0 is defined by the $1/e$ point of the complex degree of coherence [3] and $D(\rho_0, L) = 2$.

Based on the approximation expression of the WSF for the plane waves defined in Equation (19), the new SCR expression of plane waves for the case of $L_0 = \infty$ is derived, and it is defined as follows:

$$ \rho_0 \equiv \rho_{\mathrm{pl}} \approx \begin{cases} \left\{\dfrac{2^{\alpha-2}\Gamma(\alpha/2)}{\Gamma(1-\alpha/2)}\left[\tilde{\kappa}_m^{2-\alpha}\Gamma\left(1-\dfrac{\alpha}{2}\right) - \dfrac{2}{R(\alpha)\tilde{\sigma}_R^2(\alpha)}\right]\right\}^{1/(\alpha-2)}, & l_0<<\rho_{\mathrm{pl}}<<L_0, \\ \left\{R(\alpha)\tilde{\sigma}_R^2(\alpha)\dfrac{2-\alpha}{16}\tilde{\kappa}_m^{4-\alpha}\Gamma\left(1-\dfrac{\alpha}{2}\right)\right\}^{-1/2}, & \rho_{\mathrm{pl}}<<l_0<<L_0. \end{cases} \quad (23) $$

Similarly, based on the approximation expression of the WSF for the spherical waves defined in Equation (20), the new SCR expression of the spherical waves for the case of $L_0 = \infty$ is derived, and it is defined as follows:

$$ \rho_0 \equiv \rho_{\mathrm{sp}} \approx \begin{cases} \left\{\dfrac{(\alpha-1)2^{\alpha-2}\Gamma(\alpha/2)}{\Gamma(1-\alpha/2)}\left[\tilde{\kappa}_m^{2-\alpha}\Gamma\left(1-\dfrac{\alpha}{2}\right) - \dfrac{2}{R(\alpha)\tilde{\sigma}_R^2(\alpha)}\right]\right\}^{1/(\alpha-2)}, & l_0<<\rho_{\mathrm{sp}}<<L_0, \\ \left\{R(\alpha)\tilde{\sigma}_R^2(\alpha)\dfrac{2-\alpha}{48}\tilde{\kappa}_m^{4-\alpha}\Gamma\left(1-\dfrac{\alpha}{2}\right)\right\}^{-1/2}, & \rho_{\mathrm{sp}}<<l_0<<L_0, \end{cases} \quad (24) $$

while $\alpha = 11/3$ and $\zeta = 1$, which makes a special case of the well-known isotropic Kolmogorov turbulence, Equations (23) and (24) can be reduced to the expressions as follows:

$$ \rho_0 \equiv \rho_{\mathrm{pl}} \approx \begin{cases} \left(1.46\tilde{C}_n^2 k^2 L\right)^{-3/5}, & l_0<<\rho_{\mathrm{pl}}<<L_0, \\ \left(1.64\tilde{C}_n^2 k^2 L l_0^{-1/3}\right)^{-1/2}, & \rho_{\mathrm{pl}}<<l_0<<L_0, \end{cases} \quad (25) $$

$$ \rho_0 \equiv \rho_{\mathrm{sp}} \approx \begin{cases} \left(0.55\tilde{C}_n^2 k^2 L\right)^{-3/5}, & l_0<<\rho_{\mathrm{sp}}<<L_0, \\ \left(0.55\tilde{C}_n^2 k^2 L l_0^{-1/3}\right)^{-1/2}, & \rho_{\mathrm{sp}}<<l_0<<L_0, \end{cases} \quad (26) $$

and the result of Equations (25) and (26) is consistent with the research in [3].

5. Evaluations Using Numerical Analysis

Based on the above derived new analytic expressions, we analyze the wave structure function and spatial coherence radius for the plane and spherical wave propagation in anisotropic non-Kolmogorov turbulence. There are two sets of new expressions derived, and they are set for evaluation with respect to various characterizing parameters. Those are WSFs defined in Equations (12) and (15) and SCRs defined in Equations (23) and (24), respectively. We have made some general assumptions in the numerical simulations: the optical waves propagate with the generalized structure parameter $\tilde{C}_n^2 = 1.4 \times 10^{-14} m^{3-\alpha}$; the wavelength $\lambda = 1.65 \times 10^{-6}$ m; the scalar separation distance is $\rho = 3$ cm, the inner scale of the eddy size is 1 mm, and the outer scale of the eddy size is 10 m; the optical path lengths vary from 100 m to 8 km; the power law exponent α varies from 3 to 4; and the case of $l_0 < <\rho<<L_0$ is used for the SCR simulations.

5.1. Evaluations on WSFs. The first set of simulations are performed using the new expressions of wave structure function defined in Equations (12) and (15). The focus of the evaluation is to analyze the behaviors of the WSFs in terms of various characterization parameters. Those include the power law exponent α, the turbulence strength $\tilde{\sigma}_R^2$, and the anisotropic factor ζ.

Figure 1(a) shows the behavior of the WSF with respect to the increasing power law exponent α, when the anisotropic factor $\zeta = 1$, which actually makes the turbulence isotropic. The WSFs increase when α varies from 3 to 3.3 and then decrease gently afterwards. One can see the smooth bumps that the WSFs get to their maximum when $\alpha \approx 3.3$. On the other hand, Figure 1(b) shows the behaviors of the WSF with respect to the turbulence strength $\tilde{\sigma}_R^2$. The WSFs monotonically increase as the turbulence strength increases. One can observe that the values of WSF for the plane waves are always bigger than those of spherical waves in both figures.

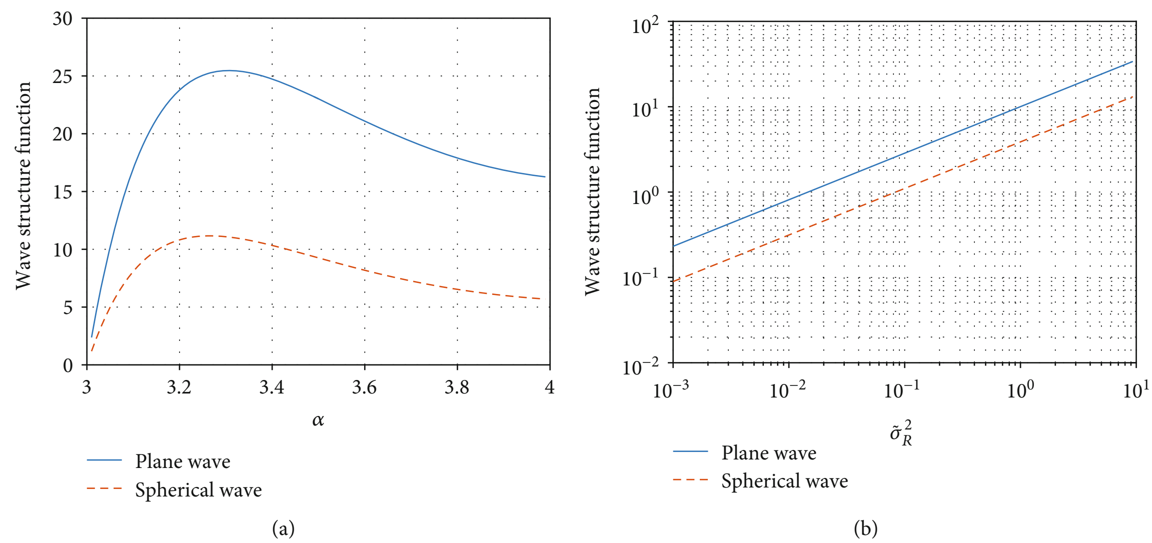

FIGURE 1: WSF as a function of increasing (a) power exponent α and (b) turbulence strength.

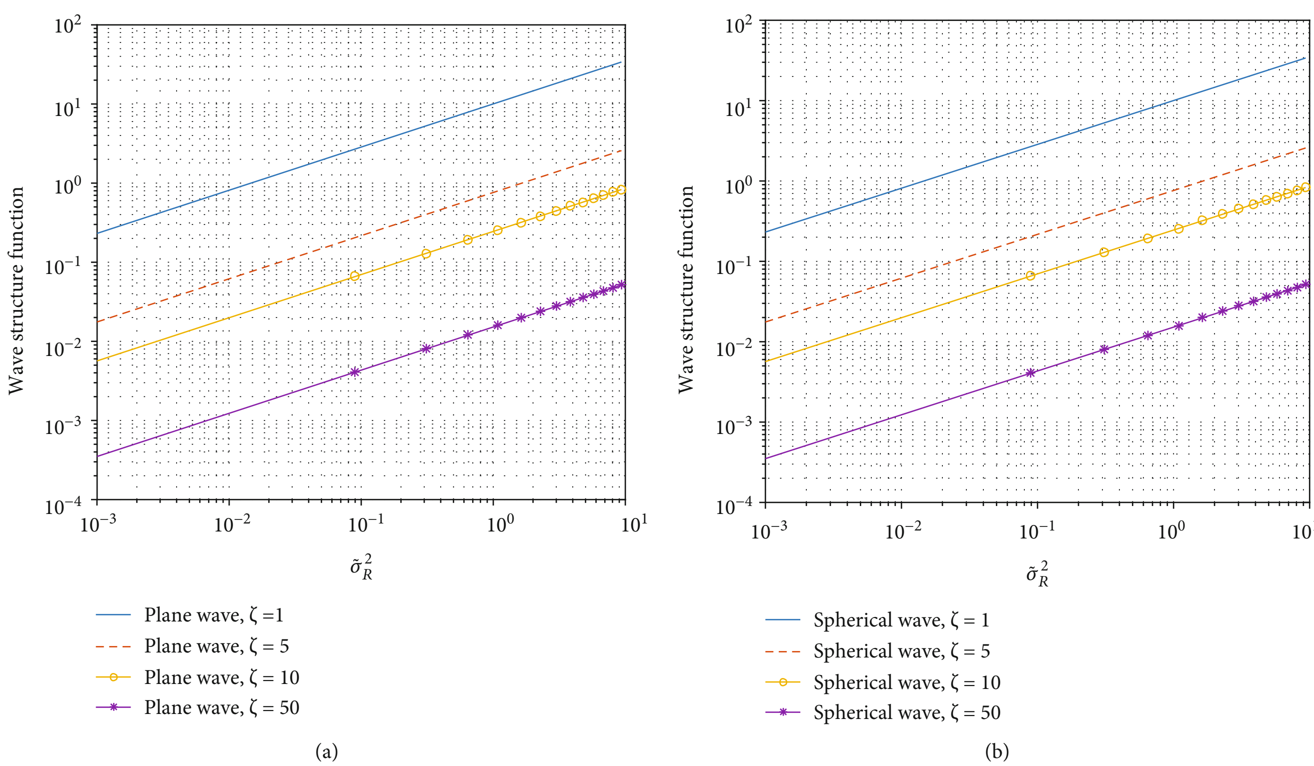

FIGURE 2: WSF as a function of increasing turbulence strength for a varying anisotropic factor: (a) plane wave and (b) spherical wave.

Figure 2 shows the behavior of the WSF with respect to the increasing turbulence strength $\tilde{\sigma}_R^2$ and the increasing anisotropic factor ζ. Figure 2(a) is for the plane waves, and Figure 2(b) is for the spherical waves. In both cases, the WSFs increase as the turbulence strength gets stronger. Also, it is also important to note that the WSFs are significantly influenced by the anisotropic factor ζ that the strength of the WSFs gets as much as 400 times weaker as the anisotropy increases from 1 to 50.

Figure 3 shows the behavior of the WSF with respect to the scales of the eddy sizes. In these simulations, we have set that the anisotropic factor $\zeta = 1$ and the power law exponent $\alpha = 11/3$. In Figure 3(a), one can observe that the WSFs for both optical waves slowly decrease as the inner scale of the eddy size l_0 increases. On the other hand, in Figure 3(b), the WSFs increase asymptotically as the outer scale of the eddy size L_0 increases. Note that the WSFs increase sheer over the outer scale of the eddy size up to 20 meters.

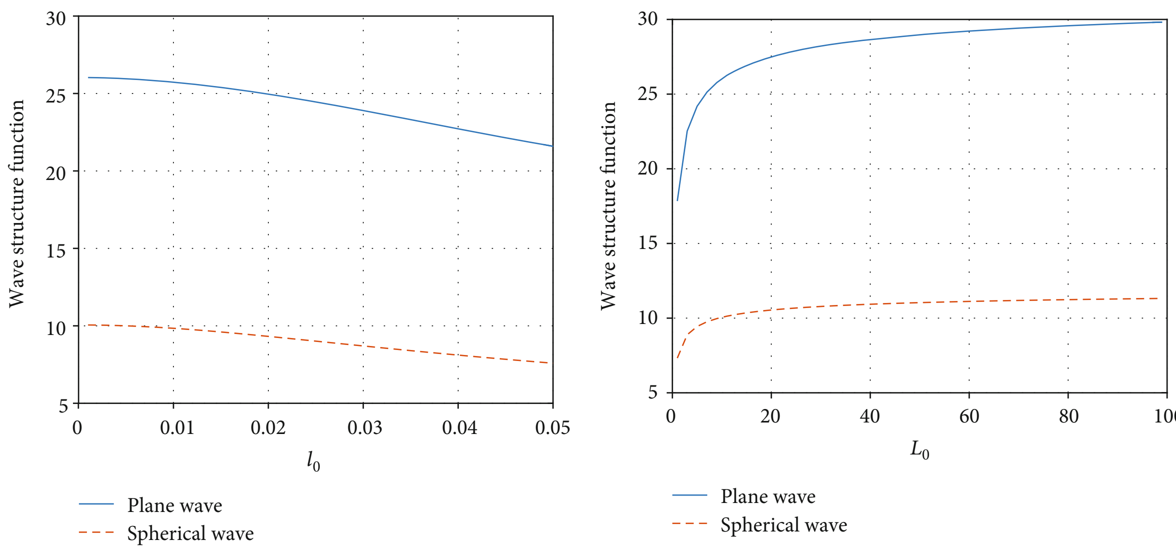

(a) (b)

Figure 3: WSF as a function of increasing the value of (a) inner scale and (b) outer scale.

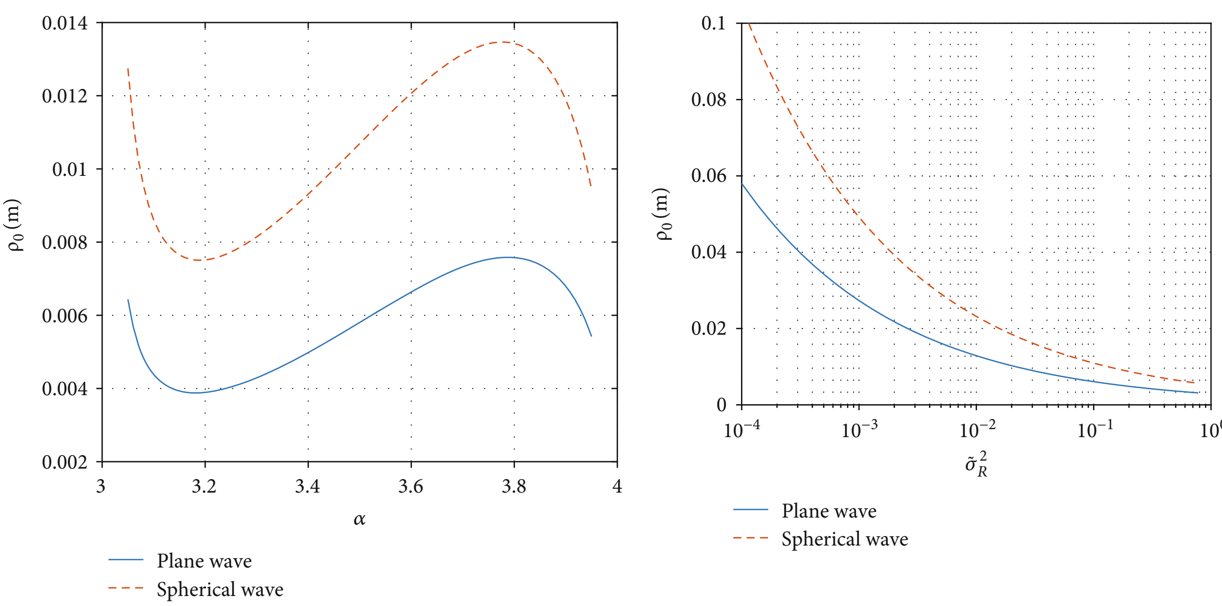

(a) (b)

Figure 4: Spatial coherence radius as a function of increasing (a) power exponent α and (b) turbulence strength.

6. Evaluation on SCRs

The second set of simulations is performed using the new expressions of spatial coherence radiuses defined in Equations (23) and (24). Similar to the simulations using the WSFs, the focus of the evaluation is also to analyze the behaviors of SCRs in terms of various characterization parameters. Those include the power law exponent α, the turbulence strength $\tilde{\sigma}_R^2$, and the anisotropic factor ζ.

Figure 4(a) shows the behavior of the SCR with respect to the increasing power law exponent α when the anisotropic factor $\zeta = 1$, which actually makes the turbulence isotropic. Power law exponent α is related to altitude of the propagation path of optical waves [34]. It is clear that the height will influence the atmosphere condition and the curves change when the atmosphere changes. The SCRs decrease sheer when α varies from 3 to 3.2 and increase gently when α varies from 3.3 to 3.8 and finally decrease sheer afterwards as α goes to 4. On the other hand, Figure 4(b) shows the behavior of the SCR with respect to the turbulence strength $\tilde{\sigma}_R^2$. The SCRs also monotonically decrease as the turbulence strength increases. It is notable that the strengths of SCRs for two optical waves become almost the same when the turbulence strength gets moderate to strong, i.e., $\tilde{\sigma}_R^2 >> 1$. The physical

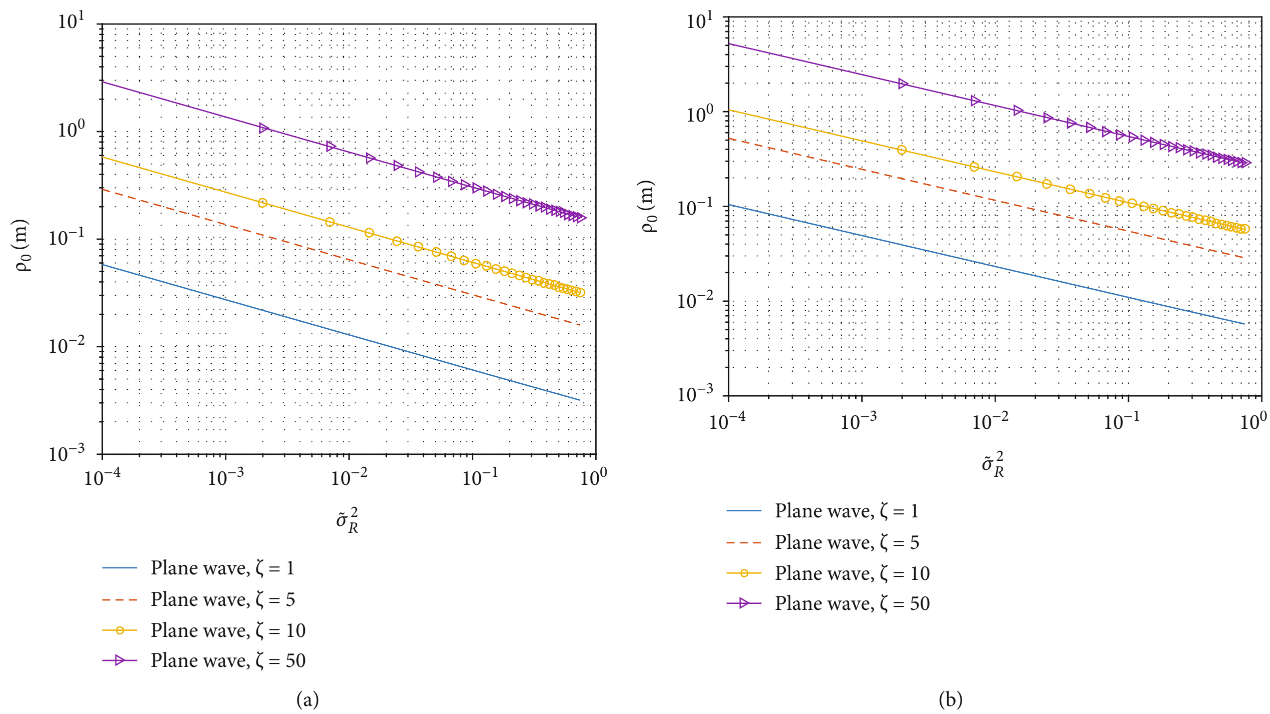

FIGURE 5: Spatial coherence radius as a function of increasing turbulence strength for a varying anisotropic factor: (a) plane wave and (b) spherical wave.

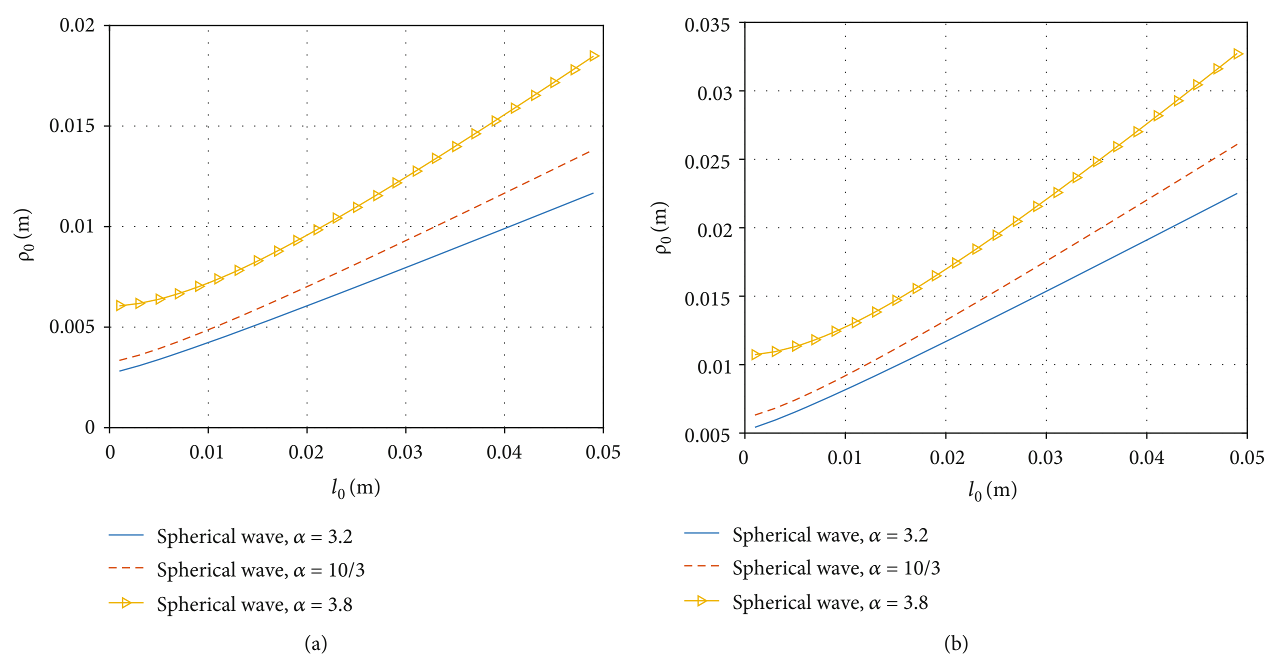

FIGURE 6: Spatial coherence radius as a function of increasing inner scale for a varying power exponent: (a) plane wave and (b) spherical wave.

reason for this phenomenon is that the strong turbulence will weaken the optical wave signals; thus, the SCR will reduce when the turbulence strength increases. Moreover, as in the simulations using the SCRs, the magnitudes of the plane waves are always smaller than those of the spherical waves.

Figure 5 shows the behavior of the SCR with respect to the increasing turbulence strength $\tilde{\sigma}_R^2$ and the increasing anisotropic factor ζ. Figure 5(a) is for the plane waves, and Figure 5(b) is for the spherical waves. On the contrary to the WSF cases, the SCRs decrease as the turbulence strength gets stronger. Also, it is important to note that the SCRs are also significantly influenced by the anisotropic factor ζ that the strength of the SCRs gets as much as 40 times stronger as the anisotropy increases from 1 to 50. The physical reason for this can be found in the anisotropic property of eddies; the eddies work as lenses with a larger radius of curvature in anisotropic turbulence than in isotropic turbulence, and the larger curvature lenses can focus an optical wave better than in isotropic turbulence [35].

Finally, Figure 6 shows the behavior of the SCR with respect to the inner scale of the eddy size l_0. In these simulations, we have set that the anisotropic factor $\zeta = 1$ and the power law exponent α equals to 3.2, 10/3, and 3.8, respectively. The simulation results show that the SRCs for both of the optical waves are significantly influenced by the inner scale of the eddy size; the curves increase monotonically as l_0 increases. Moreover, the plane waves are more affected by the power exponent factor α at the fixed inner scale of the eddy size; its magnitude increases as much as 50 percent as varies from 3.2 to 3.8. As the SCR gets smaller, it means the receiver needs more work to equalize the channel distortion.

7. Conclusion

In this work, we have presented new sets of expressions for the wave structure functions and also for the spatial coherence radiuses of the free-space optical waves such as the plane waves and the spherical waves propagating in a horizontal path of a free space, which is disturbed by anisotropic turbulence. Those newly derived analytic expressions of WSFs and SCRs are evaluated, and their behaviors are observed by varying five major characterizing parameters, which are the power law exponent α, the turbulence strength $\tilde{\sigma}_R^2$, the anisotropic factor ζ, and the inner scale and the outer scale of the eddy size, l_0 and L_0, respectively.

Those five parameters individually or in their combinations have extensive impacts on the magnitudes of the WSFs and SCRs. The behaviors of the WSFs and the SCRs come out differently with respect to the power law exponent. Also, with respect to the increasing turbulence strength, the WSFs and SCRs show an inverse relation that the WSFs increase while the SCRs decrease. Similarly, the anisotropic factor affects the WSFs and the SCRs inversely. In other words, the WSFs increase as the anisotropy increases while the SCRs decrease on the contrary. Finally, the scales of the eddy size gently affect the WSFs and the SCRs that both of them monotonically increase as the scales of the eddy sizes increase regardless of the inner scale or the outer scale. Particularly, for the SCRs, the plane waves are more significantly affected by the turbulence power than the spherical waves. Moreover, the bigger power law exponents shrink the size of SCRs more than those of the smaller ones; the plane waves are also more affected than the spherical waves in this case as well.

We have also found that the wave structure function can be used to analyze the temporal frequency spreads of optical waves and MTF of an imaging system. In the optical communication system, in order to recognize the target effectively, it is necessary to evaluate the micro-Doppler shift caused by the background noise. This kind of noise also includes the wave caused by optical wave propagation in turbulent atmosphere. These random changes cause frequency spread in the spectrum of laser signal, which is manifested as additional Doppler frequency shift. In addition, the significant frequency spread can eliminate the micro-Doppler shift caused by the target. Therefore, the temporal frequency spread of optical waves can be used in lidar system, optical detection, ranging system, and other target detection and recognition fields. In conjunction with the current work presented in this paper, we are also looking at the effects of short-exposure MTFs on imaging systems of optical waves propagating in a free space with anisotropic maritime turbulence; the propagation paths can be slant and horizontal. Our results have important theoretical and practical significance for optical communication and imaging and sensing systems involving turbulent atmospheric channels on 6G communication. Also, our research has some limitations; the work is mainly based on the power-law spectrum derived from the mathematical formula and no outdoor experiments. In future work, we will try to compare the results with the measured data from the outdoor experiment, because the outdoor results can better represent the actual atmospheric conditions.

Data Availability

The data used to support the findings of this study are available from the corresponding author upon request.

Conflicts of Interest

The authors declare that there are no conflicts of interest.

Acknowledgments

This work was supported by the Science and Technology Planning Project of Guangdong Province of China (Grant No. 2020A1414010285), the Natural Science Foundation of Jiangsu Province of China (Grant No. BK20201201), the Brain Korea 21 Program for Leading Universities & Students, the Professorial and Doctoral Scientific Research Foundation of Applied Technology College of Soochow University, Suzhou (Grant No. RC0006), and the Professorial and Doctoral Scientific Research Foundation of Huizhou University (Grant Nos. 2020JB014 and 2019JB019).

References

[1] C. Uysal, B. Ghassemlooy, and E. G. Udvary, *Optical wireless communications- an emerging technology*, Springer Publishing Company, 2016.

[2] Z. Ghassemlooy, W. Popoola, and S. Rajbhandari, *Optical Wireless Communications : System and Channel Modelling with MATLAB*, CRC Press, Inc., 2012.

[3] L. C. Andrews and R. L. Phillips, *Laser Beam Propagation through Random Media*, SPIE Press, Bellingham, WA, USA, 2005.

[4] V. I. Tatarskii, *The Effects of the Turbulent Atmosphere on Wave Propagation*, Israel Program for Scientific Translations, Jerusalem, Israel, 1971.

[5] A. Ishimaru, *Wave Propagation and Scattering in Random Media*, John Wiley & Sons, 1999.

[6] I. Toselli, L. C. Andrews, R. L. Phillips, and V. Ferrero, "Angle of arrival uctuations for free space laser beam propagation through non Kolmogorov turbulence," in *Atmospheric Propagation IV*, no. article 65510E, 2007International Society for Optics and Photonics, 2007.

[7] I. Toselli, "Introducing the concept of anisotropy at different scales for modeling optical turbulence," *Josa A*, vol. 31, no. 8, p. 1868, 2014.

[8] L. Cui, B. Xue, and F. Zhou, "Generalized anisotropic turbulence spectra and applications in the optical waves propagation through anisotropic turbulence," *Optics Express*, vol. 23, no. 23, 2015.

[9] Y. Baykal, "Intensity fluctuations of asymmetrical optical beams in anisotropic turbulence," *Applied Optics*, vol. 55, no. 27, p. 7462, 2016.

[10] Y. Baykal, Y. Luo, and X. Ji, "Scintillations of higher order laser beams in anisotropic atmospheric turbu-lence," *Applied Optics*, vol. 55, no. 33, p. 9422, 2016.

[11] J. Ma, Y.-L. Fu, S.-Y. Yu, X. Xie, and L. Tan, "Further analysis of scintillation index for a laser beam propagating through moderate-to-strong non-kolmogorov turbulence based on generalized effective atmospheric spectral model," *Chinese Physics B*, vol. 27, no. 3, article 034201, 2018.

[12] J. M. Cheng, L. Guo, J. Li, X. Yan, R. Sun, and Y. You, "Effects of asymmetry atmospheric eddies on spreading and wander of bessel-gaussian beams in anisotropic turbulence," *IEEE Photonics Journal*, vol. 10, no. 3, pp. 1–10, 2018.

[13] L. Tang, H. Wang, X. Zhang, and S. Zhu, "Propagation properties of partially coherent Lommel beams in non-Kolmogorov turbulence," *Optics Communications*, vol. 427, pp. 79–84, 2018.

[14] L. Andrews, W. Miller, and J. Ricklin, "Spatial coherence of a gaussian-beam wave in weak and strong optical turbulence," *The Journal of the Optical Society of America A*, vol. 11, no. 5, pp. 1653–1660, 1994.

[15] W. Wen, Y. Jin, M. Hu et al., "Beam wander of coherent and partially coherent airy beam arrays in a turbulent atmosphere," *Optics Communications*, vol. 415, pp. 48–55, 2018.

[16] Y. Jin, M. Hu, M. Luo et al., "Beam wander of a partially coherent airy beam in oceanic turbulence," *Journal of the Optical Society of America. A*, vol. 35, no. 8, pp. 1457–1464, 2018.

[17] G. Wu, W. Dai, H. Tang, and H. Guo, "Beam wander of random electromagnetic Gaussian-Shell model vortex beams propagating through a Kolmogorov turbulence," *Optics Communications*, vol. 336, pp. 55–58, 2015.

[18] J. Strohbehn and S. Clifford, "Polarization and angle-of-arrival fluctuations for a plane wave propagated through a turbulent medium," *IEEE Transactions on Antennas and Propagation*, vol. 15, no. 3, pp. 416–421, 1967.

[19] X. Ke and Z. Tan, "Effect of angle-of-arrival fluctuation on heterodyne detection in slant atmospheric turbulence," *Applied Optics*, vol. 57, no. 5, pp. 1083–1090, 2018.

[20] J. Borgnino, F. Martin, and A. Ziad, "Effect of a finite spatial-coherence outer scale on the covariances of angle- of-arrival fluctuations," *Optics Communications*, vol. 91, no. 3-4, pp. 267–279, 1992.

[21] B. Guan and J. Choi, "Temporal frequency spread of optical waves propagating in anisotropic maritime atmospheric turbulence," *Applied Optics*, vol. 58, no. 11, pp. 2913–2919, 2019.

[22] C. Young, A. J. Masino, F. E. Thomas, and C. J. Subich, "The wave structure function in weak to strong fluctuations: an analytic model based on heuristic theory," *Waves in Random Media*, vol. 14, no. 1, pp. 75–96, 2004.

[23] R. L. Lucke and C. Y. Young, "Theoretical wave structure function when the effect of the outer scale is significant," *Applied Optics*, vol. 46, no. 4, p. 559, 2007.

[24] X. Ji, X. Li, and G. Ji, "Propagation of second-order moments of general truncated beams in atmospheric turbulence," *New Journal of Physics*, vol. 13, no. 10, article 103006, 2011.

[25] L. Lu, X. Ji, and Y. Baykal, "Wave structure function and spatial coherence radius of plane and spherical waves propagating through oceanic turbulence," *Optics Express*, vol. 22, no. 22, pp. 27112–27122, 2014.

[26] L. Cui, B. Xue, X. Cao, and F. Zhou, "Atmospheric turbulence MTF for optical waves′ propagation through anisotropic non-Kolmogorov atmospheric turbulence," *Optics & Laser Technology*, vol. 63, pp. 70–75, 2014.

[27] L. Cui and B. Xue, "Influence of anisotropic turbulence on the long-range imaging system by the MTF model," *Infrared Physics & Technology*, vol. 72, pp. 229–238, 2015.

[28] S. Kotiang and J. Choi, "Wave structure function and long-exposure MTF for laser beam propagation through non-Kolmogorov turbulence," *Optics & Laser Technology*, vol. 74, pp. 87–92, 2015.

[29] B. Guan, H. Yu, W. Song, and J. Choi, "Wave structure function and long-exposure MTF for Gaussian-beam waves propagating in anisotropic maritime atmospheric turbulence," *Applied Sciences*, vol. 10, no. 16, p. 5484, 2020.

[30] B. E. Stribling, B. M. Welsh, and M. C. Roggemann, "Optical propagation in non-Kolmogorov atmospheric turbulence," in *Atmospheric Propagation and Remote Sensing IV*, vol. 2471, pp. 181–197, International Society for Optics and Photonics, 1995.

[31] S. Kotiang and J. Choi, "Temporal frequency spread of optical wave propagation through anisotropic non-Kolmogorov turbulence," *Journal of Optics*, vol. 17, no. 12, article 125606, 2015.

[32] L. C. Andrews, *Special Functions of Mathematics for Engineers*, McGraw-Hill, 2nd ed edition, 1997.

[33] I. Toselli, L. C. Andrews, R. L. Phillips, and V. Ferrero, "Scintillation index of optical plane wave propagating through non-Kolmogorov moderate-strong turbulence," in *Optics in Atmospheric Propagation and Adaptive Systems X*, vol. 6747, International Society for Optics and Photonics, 2007.

[34] A. Zilberman, E. Golbraikh, and N. S. Kopeika, "Propagation of electromagnetic waves in Kolmogorov and non-Kolmogorov atmospheric turbulence: three-layer altitude model," *Applied Optics*, vol. 47, no. 34, pp. 6385–6391, 2008.

[35] I. Toselli, B. Agrawal, and S. Restaino, "Light propagation through anisotropic turbulence," *JOSA A*, vol. 28, no. 3, p. 483, 2011.